RSC Advances

PAPER

Cite this: *RSC Adv.*, 2015, **5**, 75395

Ambient *in situ* analysis and imaging of both hydrophilic and hydrophobic thin layer chromatography plates by electrostatic spray ionization mass spectrometry†

Xiaoqin Zhong,[a] Liang Qiao,[a] Baohong Liu[b] and Hubert H. Girault*[a]

Received 9th June 2015
Accepted 1st September 2015

DOI: 10.1039/c5ra10977a

www.rsc.org/advances

Electrostatic spray ionization (ESTASI) mass spectrometry imaging (MSI), recently developed to profile spatial distribution of chemical and biochemical molecules on an insulating surface under ambient conditions, has been applied to identify and quantify chemicals from silica gel surfaces. Both hydrophilic or hydrophobic silica plates have been imaged with good resolution providing a direct identification of the samples. For the hydrophilic silica gel substrate, silanization of the plate before ESTASI-MS analysis was used to render the surface hydrophobic. ESTASI-MSI is shown to be a sensitive technique for the identification of a wide range of molecules of different polarities and chemical structures with minimal sample consumption in the femtomole range.

Introduction

Compared to vacuum ionization mass spectrometry imaging (MSI), ambient ionization MSI holds the advantages of minimal sample preparation, more flexible device design and *in situ* analysis. The commonly used ambient ionization methods for MSI include desorption electrospray ionization (DESI),[1] laser ablation electrospray ionization (LAESI), desorption atmospheric pressure photoionization (DAPPI),[2] laser desorption atmospheric pressure chemical ionization (LD-APCI),[3] low-temperature plasma (LTP) mass spectrometry,[4] and liquid extraction surface analysis.[5] Recently, we have developed a novel ambient MSI system based on the newly introduced technology named electrostatic spray ionization (ESTASI)[6] and successfully imaged dried peptide spots and black dye patterns on polyimide (PI) substrates.[7] However, a major problem of ESTASI-MSI has been the low spatial resolution due to the tailing effect resulting from droplet based extraction of the weakly bound samples on insulating polymer substrates. We here show that this drawback can be circumvented when imaging thin-layer chromatography (TLC) plates by ESTASI-MSI. The strong hydrophobic or hydrophilic affinity between samples and substrates minimizes the tailing effect. By optimizing the extraction buffer conditions, selective sampling from the substrates can be realized.

TLC, one of the earliest forms of chromatography for the separation of a wide range of samples,[8–12] is still widely used nowadays in food analysis, pharmaceutical research, forensic science, biochemistry, clinical chemistry, *etc.* The compounds separated by TLC are amenable to the post-chromatographic detection and profiling by typical methods such as optical visualization and spectroscopic measurements. However, these detection methods usually have poor specificity and are restricted by the chemical or optical properties of analytes. For these reasons, mass spectrometry (MS) is a suitable technique to couple with TLC due to its rapid analysis, high specificity and structural characterization ability.[13,14] Various vacuum-based desorption ionization techniques have been applied to sample and ionize nonvolatile or thermally labile compounds directly from TLC surfaces.[15–20] Nevertheless, the widespread application of vacuum-based TLC-MS techniques has been hindered by several problems such as the requirement of a high-vacuum apparatus, difficult detection of volatile or semi-volatile compounds and interference of matrix ions in the low mass range (<700 Da) during the matrix-assisted laser desorption/ionization (MALDI) MS analysis. Interfacing TLC with ambient ionization MS without much sample pretreatment prior to MS analysis is more convenient in the view of fast analysis. Recently, several ambient ionization methods, including electrospray ionization (ESI) based techniques,[21–27] APCI,[28] DART[29] and inductively coupled plasma ICP[30,31] have been introduced for the direct coupling of TLC with MS. Among the ambient MS methods, DESI-MS is a powerful one and has been coupled with TLC since 2005, where the primary charged solvent droplets produced by electrospray ionization were directed to a TLC plate to sample and ionize the analytes.[24] Then a closely related

[a]*Laboratoire d'Electrochimie Physique et Analytique, Ecole Polytechnique Fédérale de Lausanne, Industrie 17, CH-1951 Sion, Switzerland. E-mail: hubert.girault@epfl.ch; Fax: +41 21 693 3667; Tel: +41 21 693 3143*

[b]*Chemistry Department, Fudan University, 220 Handan Road, 200433 Shanghai, China*

† Electronic supplementary information (ESI) available. See DOI: 10.1039/c5ra10977a

approach, named nano-DESI, was developed in 2010, which enables the separation of desorption and ionization events by using two capillaries to form a solvent bridge to desorb analytes from substrates followed by ionization through self-aspirating nanoelectrospray.[27] Tissue imaging was demonstrated by using this technique with good spatial resolution and high sensitivity.[32]

In this work, ESTASI is coupled with TLC directly. Sample spots separated by TLC were profiled by ESTASI-MSI, including drug molecules on normal phase silica TLC plates and dyes on high performance reverse phase (HPRP) C18 silica plates. In the former case, the highly hydrophilic silica plates were modified by chlorotrimethylsilane after TLC separation to form hydrophobic surfaces for ESTASI-MS analyses. The HPRP C18 and the modified normal phase silica plates provide ideal substrates for *in situ* characterization and accurate sample location by ESTASI-MS with efficient sample extraction, reduced tailing effect due to the hydrophobic–hydrophobic or hydrophilic–hydrophilic interactions between samples and TLC substrates and even the abilities of sample desalting to enhance the detection sensitivity. The TLC-ESTASI-MS is universal for a wide range of organic molecules with very different chemical properties and polarities. The sample consumption can be as low as 75 fmol of fluorescein on the HPRP C18 plate, or ≤33 fmol of enrofloxacin on the normal phase silica plate. In addition to the identification of sample spots, the TLC-ESTASI-MS strategy can also provide a separation profile of the samples on the plates in a line-scan mode, or even a distribution image of the spots in a 2D-scan mode, which is of great value when the samples are colourless and do not give a clear image under UV illumination on the TLC plates with fluorescent indicators.

Experimental

Materials and methods

Methanol (99.9% HPLC grade), acetic acid (>99.9%), 4-acetamidophenol (98%), aspirin (99%) and chlorotrimethylsilane (≥98% GC grade) were obtained from Sigma-Aldrich (Schnelldorf, Switzerland). 25% aqueous ammonia and tetrahydrofuran (99.8%) were from VWR (Nyon, Switzerland). Ammonium acetate (98%) was obtained from Merck (Zug, Switzerland). Rhodamine B (99%), rhodamine 6G (99%), caffeine (98.5%), formic acid (99%) and acetonitrile (99.9% HPLC grade) were purchased from Acros Organics (Geel, Belgium). Fluorescein (Reag. Ph. Eur.), methylene blue (95%), sudan III (≥96%), crystal violet (AR grade) and ethyl acetate (99.9% HPLC grade) were obtained from Fluka (St. Gallen, Switzerland). Enrofloxacin (ENR, 98%), fleroxacin (FLE, 98%) and lomefloxacin (LOM, 98%) were purchased from TCI (Tokyo, Japan). Angiotensin I (NH_2–DRVYIHPFHL–COOH, 98%) was obtained from Bachem (Bubendorf, Switzerland). Deionized water (18.2 MΩ cm) was purified by an alpha Q Millipore system (Zug, Switzerland) and used in all aqueous solutions.

Silica TLC plates (20 cm × 20 cm, 200 μm layer thickness, PET foil base (0.4 mm thickness) with fluorescent indicator 254 nm) were purchased from Fluka (St. Gallen, Switzerland). HPRP C18 plates (10 cm × 10 cm, 200 μm layer thickness, glass plate (1.2 mm thickness) with fluorescent indicator 254 nm) were obtained from Merck (Zug, Switzerland).

Thin-layer chromatography

For the TLC-ESTASI-MS analyses of drugs (ENR, 4-acetamidophenol, aspirin, caffeine, LOM or FLE), 1 μL of sample solution (in methanol with a concentration of 0.5 mg mL^{-1}) was deposited on a silica TLC plate and developed under the mobile solution composed of methanol, 25% aqueous ammonia, ethyl acetate and acetonitrile (1 : 1 : 2 : 1 by volume). In the analysis of a drug mixture, an aqueous droplet (1 μL) containing ENR (1.4 nmol) and acetaminophen (3.3 nmol) was spotted on a silica TLC plate for the separation with the mobile solution as reported.[33]

For the TLC-ESTASI-MS analyses of dyes (fluorescein, rhodamine B, rhodamine 6G, sudan III, methylene blue or crystal violet), HPRP C18 plates were used. In the analysis of a dye mixture, a droplet (1 μL) of the dye mixture (1.7 nmol of methylene blue, 1 nmol of rhodamine 6G and 1.5 nmol of fluorescein) was spotted on a HPRP C18 plate, and developed with the mobile phase composed of methanol, tetrahydrofuran (60 : 40 by volume) and 100 mM ammonium acetate as reported.[21]

Modification and characterization of TLC plates

After sample separation, the silica gel TLC plates were coated by chlorotrimethylsilane to form hydrophobic surfaces. During the coating procedure, both a dry silica plate and a small bottle with 2 mL of chlorotrimethylsilane were placed inside a closed plastic box and all together in a fume hood overnight (~16 hours). The chlorotrimethylsilane was evaporated from the small bottle to react with silicon hydroxyl of the TLC plate. Afterwards, the modified plate was taken out of the box and placed in the fume hood for another 1 h to let the excess chlorotrimethylsilane vapour evacuate.

Characterization of the modified and unmodified silica TLC and the HPRP C18 plate was performed by a Drop Shape Analysis System DSA100 from Krüss GmbH (Hamburg, Germany), where the contact angles of different solvents on the plates were tested.

ESTASI-MS

The mass spectrometer used to detect ions produced by ESTASI was a linear ion trap (Thermo LTQ Velos), where the MS inlet was always grounded and the positive ion-scanning mode was chosen. The ESI voltage of the internal power source of the MS instrument was always set as 0 during ESTASI-MS experiments. The enhanced ion trap scanning rate of 10 000 mass-to-charge ratio (m/z) per second was used.

The ESTASI setup was illustrated in Fig. 1. High voltage pulses (from 0 V up to 9 kV, 20 Hz) were generated by amplifying square wave voltage pulses with a high voltage amplifier (10HVA24-P1, HVP High Voltage Products GmbH, Martinsried/Planegg, Germany) to induce the ESTASI. A self-designed ion transfer capillary in "L" shape (2 mm of outer diameter (o.d.), 0.8 mm of inner diameter (i.d.)) replaced the original one for

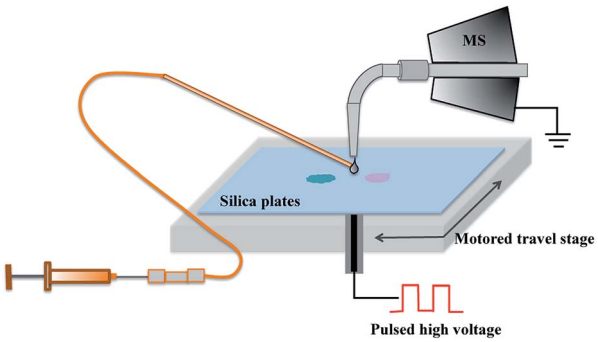

Fig. 1 Schematic representation of the setup used for TLC-ESTASI-MS.

convenient scan of a horizontally placed surface. A TLC plate containing sample spots was supported on a thin insulating polymer substrate (PET, 0.2 mm thickness) and placed under the ion transfer capillary. The TLC plate was moved by two motored travel stages (MTS50-Z8, Thorlabs, Dachau/Munich, Germany) in x and y directions to bring the sample spots under the MS inlet for detection, linear scans or 2D MSI. A fused silica capillary (150 μm o.d., 50 μm i.d.) named wetting capillary was in contact with the TLC plate surface to deliver acidic solvent for sample extraction and ionization.

Several parameters were adjusted precisely to obtain good MS signals, including the distance between the sample surface and the ion transfer capillary, the angle between the fused silica capillary and the sample surface, the flow rate of the acidic solvent and the solvent component.

ESTASI-MS selected reaction monitoring (SRM) was performed by collision induced dissociation (CID) with normalized collision energy of 25. The isolation width of precursor ion was set as ±1 m/z and the scan range of SRM was set as ±16 m/z.

Data analysis was performed by Xcalibur Qual Browser (ThermoFisher Scientific, Reinach, Switzerland). The line-scan results and mass spectra were plotted by IGOR Pro (Version 6.00 for Macintosh, WaveMetrics, Lake Oswego, OR, USA). 2D MS image and 3D TLC-ESTASI-MS map were plotted by the data processing software MIRA (G. Wittstock, University of Oldenburg; http://www.uni-oldenburg.de/chemie/pc2/pc2forschung/secm-tools/mira/).

Results and discussion

ESTASI-MS analyses of samples from HPRP C18 plates

In TLC-ESTASI-MS, a wetting capillary was used to deliver extraction solution to a TLC plate locally, and extract samples from the plate. ESTASI-MS analysis[7] of the samples can be accomplished only when the extraction solvent can establish a droplet under the MS inlet and when the samples can be efficiently extracted into the droplet. Thus, the extracting solvent needs to be well chosen to combine a good solubility for the analytes and a good wettability for the TLC plates. For different samples and TLC plates, the different solvent composition should be optimized accordingly.

One typical application of the TLC-ESTASI-MS system is based on reverse phase TLC plates. In this work, a HPRP C18 plate was selected, because of its excellent separation ability with respect to various organic molecules, and its highly hydrophobic surface property. Several identical sample droplets (1 μL, 0.3 mM fluorescein) were deposited on a HPRP C18 plate and then developed in parallel by the mobile solution of methanol and tetrahydrofuran (60 : 40 v/v) with 100 mM ammonium acetate to obtain several sample spots with the size of ~5 mm in diameter each. Five extraction solvents, containing 0%, 25%, 50%, 75% and 99% H_2O respectively, in methanol with 1% acetic acid were tested. Sampling with each solvent lasted for 30 s on the centre of the fluorescein spot with continuous ESTASI-MS detection. Due to the different absorption of the HPRP C18 plate to different extraction solvents, the injection flow rate of each solvent was adjusted to obtain the best MS signals for the solvent.

From the recorded mass spectra, ratios between the peak intensities of the fluorescein ion and the internal standard (IS) ion, which was the triply protonated Ang I, were calculated, averaged and plotted *versus* the percentages of water in the extraction solvent, as shown in Fig. 2(a). The MS intensity of fluorescein in comparison with the IS reduced greatly with the incremental change of water percentage. It is reasonable by considering that the less-polarized solvent with more methanol should have a better extraction capacity of samples from the reverse phase TLC plates, where the affinity between the samples and the C18 modified plate is based on hydrophobic–hydrophobic interactions. In spite of the largest extraction efficiency, it was difficult to form a stable ESTASI with the solvent consisting of 99% methanol and 1% acetic acid to always form a stable MS signal. Because of the relatively strong absorption of the HPRP C18 plate to methanol, the extraction solvent with 99% methanol can also induce the development of the sample in the plate, which would especially influence the linear scan or 2D imaging of TLC spots by MS. Therefore, the solvent composed of 75% methanol, 24% water and 1% acetic acid was selected for the further experiments on the HPRP C18

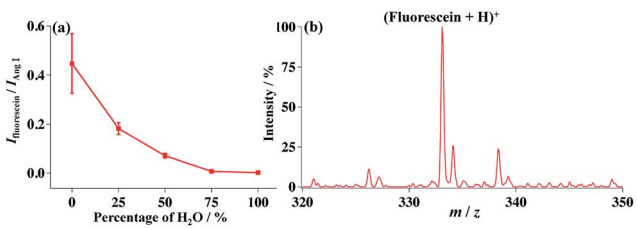

Fig. 2 Extraction solvent optimization and detection limit of fluorescein on HPRP C18 plate. (a) Optimization of the extraction solvent (water and methanol mixture with 1% acetic acid). $I_{fluorescein}$: intensity of singly protonated fluorescein at m/z = 333.3; $I_{Ang\ I}$: intensity of three-protonated angiotensin I at m/z = 432.9. (b) Mass spectrum of fluorescein detected by ESTASI-MS from the HPRP C18 plate with 1% acetic acid, 75% methanol and 24% H_2O as the extraction solvent under a flow rate of 1 μL min^{-1}. Sample on TLC: fluorescein (1 μL, 30 μM aqueous solution) developed by the mobile solution of methanol and tetrahydrofuran (60 : 40 v/v) with 100 mM ammonium acetate.

plate to evaluate the detection limit of fluorescein by TLC-ESTASI-MS.

Stock solutions with different concentrations of fluorescein were prepared. 1 μL of each was spotted on a HPRP C18 plate and then developed by the mobile phase described above to form final sample spots. The fluorescein spot dried from 1 μL of 30 μM solution could still be easily detected by ESTASI-MS with the signal-to-noise ratio (S/N) of about 12, Fig. 2(b). The spot diameter was around 5 mm, while the extraction area was about 250 μm in diameter. Accordingly, the fluorescein consumption amount was estimated to be ≤75 fmol, indicating that the HPRP C18 TLC-ESTASI-MS system is suitable for the analyses of trace analytes.

Rhodamine B, rhodamine 6G, sudan III, methylene blue and crystal violet can also be analyzed in the same way on the HPRP C18 plate by ESTASI-MS, indicating that the method is universal to a wide range of molecules with different chemical properties and polarities. The obtained mass spectra by TLC-ESTASI-MS and the structure of these molecules are shown in the ESI (S1 and S2†).

ESTASI line-scan and 2D imaging of sample spots separated by HPRP C18 plates

Based on the characterization of TLC spots by ESTASI-MS, line scan and 2D imaging of the spots were performed, which could be useful in discerning slightly overlapping spots or the analytes not readily visible on the plate. A dye mixture containing methylene blue (1.7 nmol), rhodamine 6G (1 nmol) and fluorescein (1.5 nmol) was separated by a HPRP C18 plate. The obtained dye spots were subjected to line scan and 2D imaging by ESTASI-MS. The extraction solution of 3 μM Ang I in 1% acetic acid, 75% methanol and 24% water was delivered at 1 μL min^{-1}. In the line scan, the motored travel stage moved with the step size of 100 μm, the translation rate of 5 mm s^{-1} and the delay time of 1 s to bring different regions of the TLC plate to the wetting capillary for analyses. MS signals were recorded, and the ion current (IC) ratio between target molecule and internal standard was calculated and normalized as shown in Fig. 3 for quantification.

Fig. 3(a)–(d) showed the optical image of the development lane containing methylene blue, rhodamine 6G and fluorescein spots, and the IC chromatography of each dye from ESTASI-MS line-scan. The white arrow on the optical image indicated the TLC developing direction, which was also the line-scan direction. The line scan crossed the centre of the TLC spots. Although the amount of each dye was almost the same in the mixture, the mass spectra signals varied a lot because of the different extraction and ionization efficiencies of the samples. Comparing Fig. 3(a) with Fig. 3(b)–(d), the ESTASI-MS line-scan showed the chromatography quite close to the optical image, but still with the following differences. The IC bandwidth of fluorescein in Fig. 3(d) was larger than that of the visual fluorescein spot in Fig. 3(a). From Fig. 3(c) and (d), there was a small overlap between rhodamine 6G and fluorescein spots, which could not be discerned visually from the optical image. The resolution of chromatographic

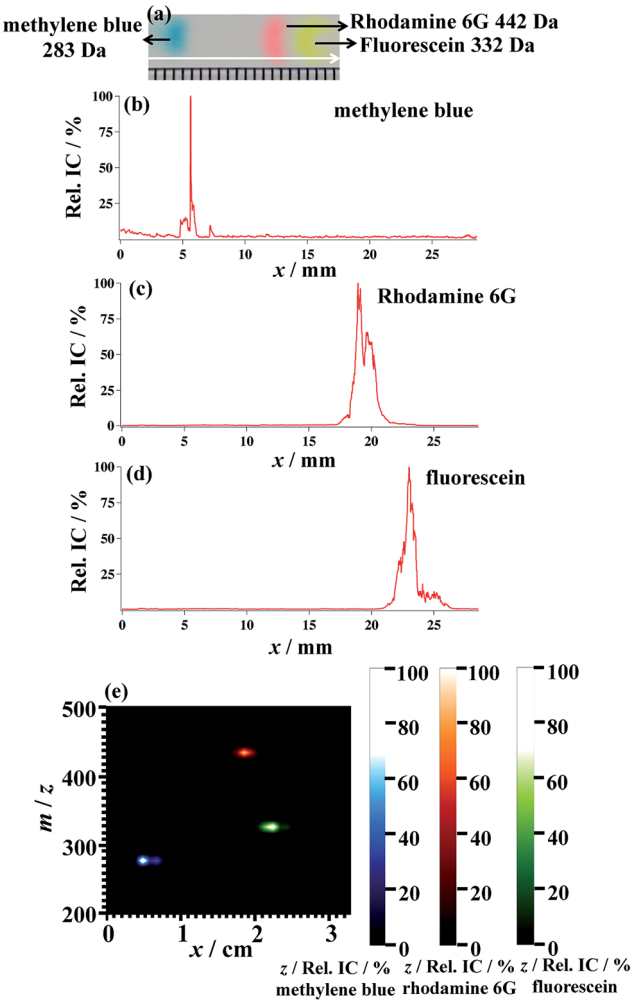

Fig. 3 ESTASI-MS line scan of a dye mixture separated on a HPRP C18 plate. The dye mixture contains methylene blue (1.7 nmol), rhodamine 6G (1 nmol) and fluorescein (1.5 nmol). (a) Optical image of the dried samples. (b), (c) and (d) normalized relative ion current (Rel. IC/%) chromatography of methylene blue, rhodamine 6G and fluorescein, respectively. (e) 3D TLC-ESTASI MS map of the three dyes. Rel. IC of each dye was calculated by dividing the IC of singly protonated sample molecule by that of the triply protonated Ang I, and then normalized, respectively.

bands in TLC was further considered to evaluate the TLC-ESTASI-MS, which is defined as the distance between the band centres divided by the average width of the bands.[12] The calculated TLC resolutions were 5.52 and 5.38 for the separation of methylene blue and rhodamine 6G, and 1.60 and 1.20 for the separation of rhodamine 6G and fluorescein, based on the optical image and ESTASI-MS, respectively. On one hand, the difference between the IC chromatography and the optical image can stem from the limited spatial resolution of ESTASI-MS, which is regulated by the wetting capillary size, and the step size. On the other hand, the optical image could hinder some details of the sample spots when their surface concentration is too low to give a colour strong enough to see, which could still be revealed by ESTASI-MS.

The main advantages of MS scan of TLC plates compared with any spectroscopy detection method are the direct characterization of analytes and the possibility to differentiate in m/z the analytes not well separated by TLC. For this purpose, a concept of 3D TLC-ESTASI-MS map is shown here, with the x-axis representing the position of the sample spot on the scanned lane, the y-axis representing the m/z ratio and the z-axis in colour gradient representing the surface density. Fig. 3(e) showed the 3D TLC-ESTASI-MS map reconstructed from the line scan MS data. There is a small degree of overlap on the x-axis between fluorescein and rhodamine 6G spots as already found in Fig. 3(c) and (d), while the spots are well separated on the 3D map by m/z that brings a great value to the TLC analyses of mixtures.

2D ESTASI-MSI was further performed on the same rhodamine 6G and fluorescein bands on the TLC plate in Fig. 3(a) with a protocol described in detail in a recent publication.[7] The same extraction solvent was used, and the motored travel stage was moved in both x and y directions with the step size of 200 μm, the translation rate of 5 mm s^{-1} and the delay time of 1 s to accomplish the 2D scan. Normalized Rel. IC of each dye was calculated and plotted *versus* the position on the TLC plate to form a 2D MS image of the dye spots, where a more bright colour means a more intensive signal of the corresponding sample on mass spectrum, shown as Fig. 4. The plotted image of the two dye spots by TLC-ESTASI-MSI was similar to the optical image. Before reaching the sample spots, only the 3 protonated Ang I was observed on the mass spectra while both 3 protonated Ang I and dye ions were observed when ESTASI-MS was performed on the corresponding dye spot (S2†). Considering that the spots had already been used for line scan before the 2D imaging, the ESTASI-MS consumed only small amount of samples for each analysis, making it possible to reanalyze the plate several times before the consumption of the entire sample. Indeed, with a sample spot of 1 μL, 10 μg mL^{-1} rhodamine 6G on a HPRP C18 plate the ESTASI-MS signal of rhodamine 6G lasted for more than 2 min with S/N > 3, where 3 μM Ang I in 1% acetic acid, 75% methanol and 24% water was delivered by the wetting capillary at 1 μL min^{-1} to extract sample continuously from the central position of the developed band, see ESI Fig. S4.† Summing all the MS signal of rhodamine 6G during the constant TLC-ESTASI-MS analysis, the recovery rate was determined as 78 ± 3.5%.

The good correspondence between Fig. 4 and 3(a) demonstrated that 2D ESTASI-MSI is a powerful method to reveal completely and accurately the spatial distribution of the analytes separated by TLC. Compared with the images obtained previously,[7] the image resolution and integrity have been improved significantly, which could be contributed to the hydrophobic–hydrophobic or hydrophilic–hydrophilic interactions between samples and TLC substrates leading to a reduced tailing effect.

Quantification capability of TLC-ESTASI-MS

Quantitative capability of TLC-ESTASI-MS was also explored by using rhodamine 6G on the HPRP C18 plate as an example. ESTASI line-scans were performed across the centre lanes of five sample bands developed on a HPRP C18 plate. The five samples were prepared from 1 μL 0.01 mg mL^{-1}, 0.05 mg mL^{-1}, 0.1 mg mL^{-1}, 0.15 mg mL^{-1} and 0.2 mg mL^{-1} rhodamine 6G, respectively. 3 μM Ang I in 1% acetic acid, 75% methanol and 24% water was delivered at 1 μL min^{-1} to extract sample for ESTASI-MS analysis. Ang I acted as internal standard for the quantification. Rel. IC was calculated as the ratio between rhodamine 6G (m/z 442.9 to m/z 443.7) and Ang I IC (m/z 432.7 to m/z 433.8). The integrated peak areas of the Rel. IC chromatography were plotted with respect to rhodamine 6G solution concentrations to obtain the calibration curve as $y = 30.666\,x - 0.105$ ($R^2 = 0.994$), in Fig. 5. Three parallel tests were performed to determine the standard deviation. A set of the Rel. IC chromatography spectra are shown in the ESI Fig. S3† as

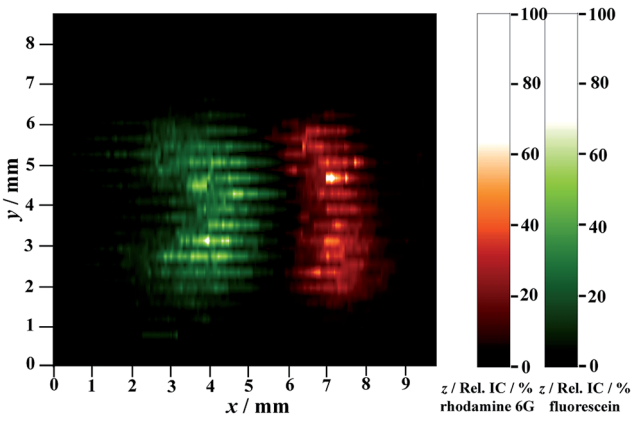

Fig. 4 2D TLC-ESTASI-MSI of rhodamine 6G and fluorescein spots in Fig. 3(a). Rel. IC/% of each dye was plotted with respect to the position on the TLC plate and represented individually as the z-axis in a form of green (fluorescein) or red (rhodamine 6G) colour gradient.

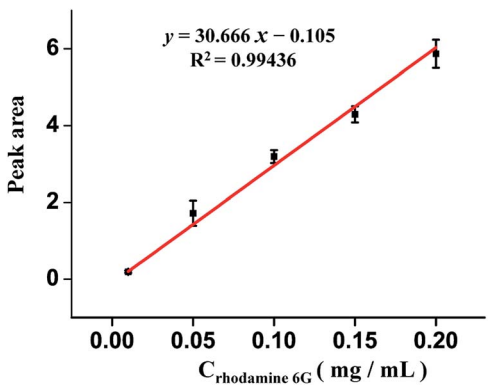

Fig. 5 Calibration plot of integrated peak area of Rel. IC chromatography of rhodamine 6G from TLC-ESTASI-MS *versus* its concentration. Each sample spot was developed from 1 μL of rhodamine 6G solutions with different concentrations, ranging from 0.01 mg mL^{-1} to 0.2 mg mL^{-1} on a HPRP C18 plate. The ESTASI was performed with the extraction solvent of Ang I (3 μM) in 1% acetic acid, 75% methanol and 24% water under the flow rate of 1 μL min^{-1}.

representative results. The results show that TLC-ESTASI-MS has a good quantification capability.

Surface modification of normal phase silica TLC plates for ESTASI-MS analyses

Solvent mixtures containing methanol, water and acetic acid are commonly used in most ESI-based MS systems. However, both water and methanol can be absorbed quickly by normal phase silica gel TLC plates without forming small droplets for the sample extraction of ESTASI-MS analysis. Furthermore, the absorbed liquid can induce sample developing inside the TLC plate. Therefore, normal phase and any water-wettable plates are very difficult to be directly analyzed by liquid-extraction based MS analysis methods. Surface modification of the plates is normally required before MS analysis. For example, silicone oil was sprayed onto the normal phase silica gel plates and HPTLC cellulose plates to form hydrophobic surfaces to enable the MS analysis by a liquid microjunction surface sampling probe.[34]

In this work, we use chlorotrimethylsilane vapour to modify silica gel TLC plates after sample separation to form highly hydrophobic surfaces for ESTASI-MS analyses. Chlorotrimethylsilane is volatile and reactive toward silicon hydroxyl groups, resulting in the replacement of the hydrophilic hydroxyl groups by hydrophobic silane. Compared to other modification procedures, such as physical cover with paraffin or silicone oil,[35] the vapour reaction of chlorotrimethylsilane with silica gel can provide a surface homogeneously modified in a thin layer, and without the coverage of the sample molecules that can lead to lower sensitivity during MS analysis. In addition, the silane does not influence MS analysis as it is chemically immobilized on the stationary phase of TLC plates that cannot be removed during ESTASI.

To evaluate the modification method, the contact angles of solvents containing different percentages of methanol and water were measured on the modified silica gel plate, the unmodified silica gel plate and the HPRP C18 plate. As shown in Fig. 6(a), the contact angles of the solvents composed of 99%, 75% and 50% water in methanol with 1% acetic acid on the silane modified silica gel plate was measured as 84°, 77° and 63°, respectively. When the water concentration was 25%, the solvent could no longer form a stable droplet. In contrast, on the silica gel plate without silane modifications, even the solvent containing 75% of water cannot form a stable droplet, Fig. 6(c). When the HPRP C18 plate was employed, the contact angles for the solvents of 99%, 75%, 50% and 25% water in methanol with 1% acetic acid were measured as 135°, 126°, 90° and 39° respectively, in Fig. 6(b). Therefore, although the silane-modified silica TLC plate is not as hydrophobic as the HPRP C18 plate, it is much more hydrophobic than the unmodified one and may be used in many liquid extraction based MS analysis methods. Because the affinity between the silica gel plate and samples is mainly based on hydrophilic–hydrophilic interactions, a higher concentration of water in the extraction solvent could benefit ESTASI-MS analysis. However, the surface tension of the solvent also increases with the amount of water,

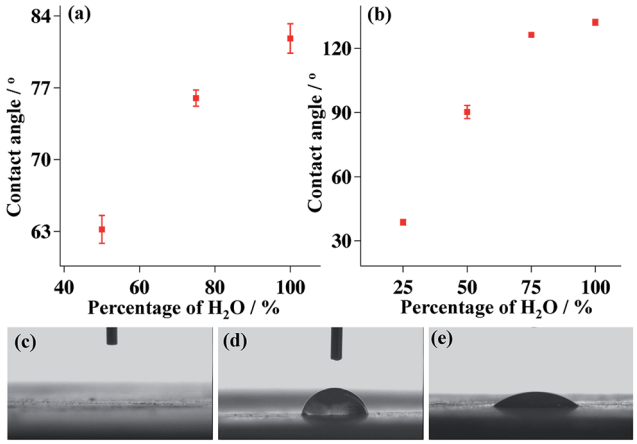

Fig. 6 Contact angles of solvents on TLC plates. (a) Contact angles of the solvents containing 50%, 75% and 99% H_2O respectively on the silane-modified silica gel TLC plate. (b) Contact angles of the solvents containing 25%, 50%, 75% and 99% H_2O respectively on the HPRP C18 plate. The error bar was obtained from three parallel tests to show the standard deviation. (c) Photograph of 75% H_2O on the silica plate. (d) Photograph of 75% H_2O on the silane-modified silica plate. (e) Photograph of 25% H_2O on a HP RP C18 plate.

making the ESTASI itself more difficult.[6] Therefore, the solvent containing 75% water, 24% methanol and 1% acetic acid was used as the extraction solvent when analyzing the silica TLC plate.

To demonstrate the effect of the silane modification in ESTASI-MS analysis, enrofloxacin (ENR), an antibiotic, was developed in parallel on two silica TLC plates by the mobile solution of methanol, 25% aqueous ammonia, ethyl acetate and acetonitrile (1 : 1 : 2 : 1 by volume), and then analyzed by ESTASI-MS, one with silane modification and the other not. In Fig. 7(a), only a weak MS peak with the S/N of about 10 and absolute intensity of 400 was observed for ENR at high amount (2.7 nmol) on the plate without modification under the extraction solvent flow rate of 2 μL min^{-1}. The high flow rate was used here to form temporarily a droplet for ESTASI-MS analysis under the strong absorption of the solvent by the TLC plate, which would induce quick diffusion of samples inside the TLC plate from the extraction droplet region. Therefore, only the spot of very high amount of ENR can be detected by ESTASI-MS. When the sample amount was lowered to 0.27 nmol, no signal of ENR was obtained from the silica gel TLC plate under optimized experimental conditions. In comparison, a much stronger MS peak of ENR with the S/N larger than 100 and absolute intensity of 10 000 was obtained from the developed sample spot containing 2.7 nmol of ENR when the silane modification was performed after TLC separation and before MS analysis, as shown in Fig. 7(b). Even when the sample amount was lowered to 14 pmol, the ENR was still detectable from the TLC plate after silane modification with the S/N of about 3 in Fig. 7(c).

It should be mentioned that the flow rate was lowered to 1 μL min^{-1} during the analyses of the silane-modified silica gel TLC plate, since the plate cannot absorb the solvent any more.

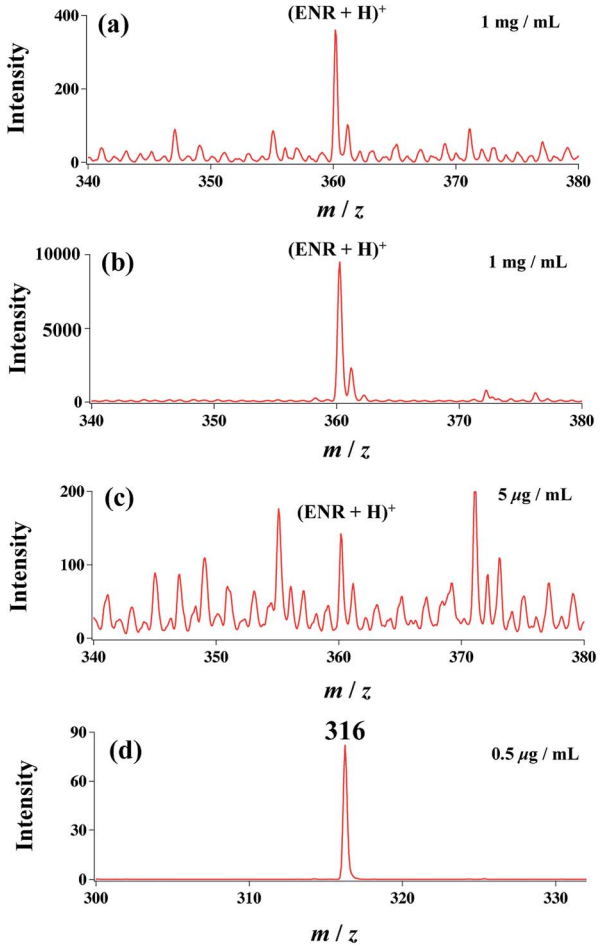

Fig. 7 ESTASI-MS spectra of sample spots from: (a) 1 μL, 1 mg mL^{-1} ENR aqueous solution developed on a silica gel TLC plate, (b) 1 μL, 1 mg mL^{-1} ENR aqueous solution developed on a silica gel TLC plate with silane modification, and (c) 1 μL, 5 μg mL^{-1} ENR solution developed on a silica gel TLC plate with silane modification. (d) ESTASI-MS SRM spectrum of a sample spot from 1 μL, 0.5 μg mL^{-1} ENR aqueous solution developed on a silica gel TLC plate followed with silane modification. ESTASI-MS was performed with the extraction solvent of 75% water, 24% methanol and 1% acetic acid. Normalized collision energy of CID: 25; isolation width of precursor ion: ±1; SRM range: *m/z* 316 ± 16.

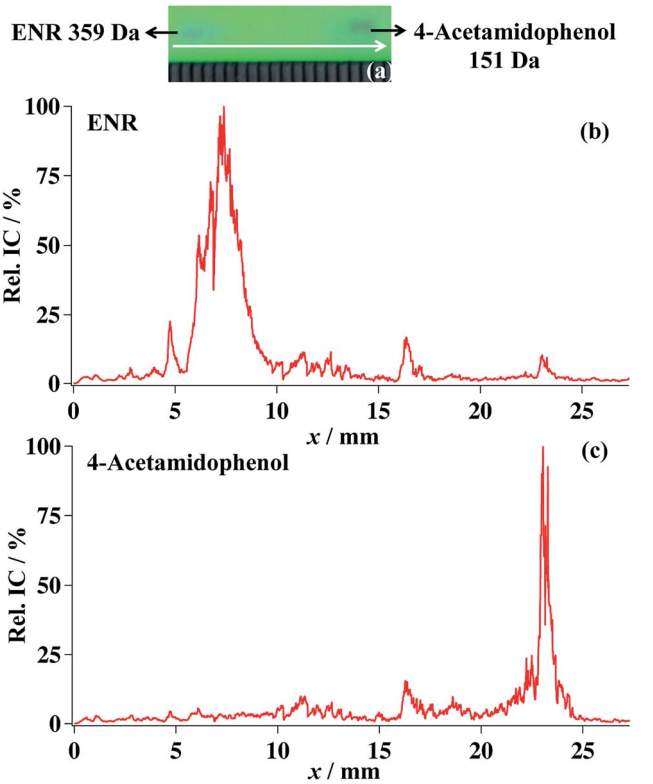

Fig. 8 ESTASI-MS line-scan of a drug mixture on a silica gel TLC plate with silane modification. The mixture contains ENR (1.4 nmol) and 4-acetamidophenol (3.3 nmol) (a) an optical image of the dried sample spots on the TLC plate. (b) and (c) Rel. IC/% chromatography of ENR and 4-acetamidophenol, respectively.

SRM analysis of ENR was also performed using a diagnostic ion at *m/z* 316, which corresponds to the neutral loss of CO_2. As shown in Fig. 7(d), the ion was still detectable with relative strong intensity (90) when the sample amount was lowered to 1.4 pmol (1 μL, 0.5 μg mL^{-1}). Since no signal at *m/z* 316 could be detected from a blank silica gel TLC plate after silane modification, the sample amount can be further lowered, indicating that the analysis specificity and sensitivity can be greatly enhanced in the SRM mode TLC-ESTASI-MS. More detailed information on TLC-ESTASI-MS SRM is given in the ESI S5.†

In the same way, we have demonstrated that 4-acetamidophenol, aspirin, caffeine, lomefloxacin and fleroxacin can also been detected by ESTASI-MS from the silica gel TLC plate after silane modification, as shown in the ESI (S1 and S6†), illustrating the universal applicability to a wide range of samples.

The line scan of sample spots on the silica gel TLC plate after silane modification can also be performed with ESTASI-MS. The drug mixture containing ENR (1.4 nmol) and 4-acetamidophenol (3.3 nmol) was separated by a silica plate. The obtained plate was then modified by silane before the ESTASI-MS line scan. The line scan was performed along the centre lane of the development bands in the developing direction indicated with a white arrow in Fig. 8(a). The extraction solution was 3 μM Ang I in 1% acetic acid, 75% water and 24% methanol, injected at the flow rate of 1 μL min^{-1}. The motored travel stage moved with the step size of 100 μm, the translation rate of 5 mm s^{-1} and the delay time of 1 s. The normalized Rel. IC of ENR and 4-acetamidophenol was calculated and plotted to form the IC chromatography, as shown in Fig. 8(b) and (c), which is in good correspondence with the optical TLC image. The TLC resolution for the separation of ENR and 4-acetamidophenol was calculated as 4.0 from the optical image and 3.8 from the ESTASI-MS chromatography.

Conclusions

In this study, we have developed a direct coupling of TLC with ESTASI-MS for *in situ* analyses under ambient conditions with no sample pretreatment. Dried samples separated by high performance reverse phase TLC plates can be analyzed and

quantified directly by ESTASI-MS. We also proposed an effective, simple surface modification process using chlorotrimethylsilane to modify hydrophilic silica gel. In a line scan mode, both chemical identification and TLC separation information can be obtained from a number of mass spectra to generate a 3D TLC-MS map. The distribution image of compounds on TLC plates can also be accomplished with a good spatial resolution in the 2D scan mode. The method was found to be appropriate to the 12 tested samples. TLC-ESTASI-MS can be readily applied in many other chemical and biochemical analyses.

Acknowledgements

Xiaoqin Zhong would like to acknowledge the China Scholarship Council for her PhD study scholarship. The authors acknowledge Yan Deng and Dr Stockmann from the Laboratoire d'Electrochimie Physique et Analytique for their helpful discussions on the manuscript. The authors acknowledge Dr Lesch from the Laboratoire d'Electrochimie Physique et Analytique for his help on the MIRA software.

Notes and references

1 Z. Takats, J. M. Wiseman, B. Gologan and R. G. Cooks, *Science*, 2004, **306**, 471–473.
2 J. Pol, V. Vidova, G. Kruppa, V. Kobliha, P. Novak, K. Lemr, T. Kotiaho, R. Kostiainen, V. Havlicek and M. Volny, *Anal. Chem.*, 2009, **81**, 8479–8487.
3 J. J. Coon, K. J. McHale and W. W. Harrison, *Rapid Commun. Mass Spectrom.*, 2002, **16**, 681–685.
4 Y. Y. Liu, X. X. Ma, Z. Q. Lin, M. J. He, G. J. Han, C. D. Yang, Z. Xing, S. C. Zhang and X. R. Zhang, *Angew. Chem., Int. Ed.*, 2010, **49**, 4435–4437.
5 G. J. van Berkel, V. Kertesz, K. A. Koeplinger, M. Vavrek and A. N. T. Kong, *J. Mass Spectrom.*, 2008, **43**, 500–508.
6 L. Qiao, R. Sartor, N. Gasilova, Y. Lu, E. Tobolkina, B. Liu and H. H. Girault, *Anal. Chem.*, 2012, **84**, 7422–7430.
7 L. Qiao, E. Tobolkina, A. Lesch, A. Bondarenko, X. Q. Zhong, B. H. Liu, H. Pick, H. Vogel and H. H. Girault, *Anal. Chem.*, 2014, **86**, 2033–2041.
8 J. Sherma, *Anal. Chem.*, 2000, **72**, 9R–25R.
9 J. Sherma, *Anal. Chem.*, 2002, **74**, 2653–2662.
10 *Thin-Layer Chromatography*, ed. H. York, W. Funk, W. Fischer and H. Wimmer, VCH, New York, 1990.
11 *Fundamentals of Thin Layer Chromatography (Planar Chromatography)*, ed. F. Geiss, Huethig, Heidelberg, 1987.
12 *Thin-Layer Chromatography*, ed. B. Fried and J. Sherma, Marcel Dekker, New York, 1999.
13 S. C. Cheng, M. Z. Huang and J. Shiea, *J. Chromatogr. A*, 2011, **1218**, 2700–2711.
14 G. Morlock and W. Schwack, *TrAC, Trends Anal. Chem.*, 2010, **29**, 1157–1171.
15 G. C. Didonato and K. L. Busch, *Anal. Chem.*, 1986, **58**, 3231–3232.
16 T. T. Chang, J. O. Lay and R. J. Francel, *Anal. Chem.*, 1984, **56**, 109–111.
17 A. J. Kubis, K. V. Somayajula, A. G. Sharkey and D. M. Hercules, *Anal. Chem.*, 1989, **61**, 2516–2523.
18 A. I. Gusev, A. Proctor, Y. I. Rabinovich and D. M. Hercules, *Anal. Chem.*, 1995, **67**, 1805–1814.
19 Y. C. Chen, J. Shiea and J. Sunner, *J. Chromatogr. A*, 1998, **826**, 77–86.
20 C. C. Chen, Y. L. Yang, C. L. Ou, C. H. Chou, C. C. Liaw and P. C. Lin, *Analyst*, 2013, **138**, 1379–1385.
21 G. J. van Berkel, A. D. Sanchez and J. M. E. Quirke, *Anal. Chem.*, 2002, **74**, 6216–6223.
22 H. Luftmann, *Anal. Bioanal. Chem.*, 2004, **378**, 964–968.
23 S. Y. Lin, M. Z. Huang, H. C. Chang and J. Shiea, *Anal. Chem.*, 2007, **79**, 8789–8795.
24 G. J. van Berkel, M. J. Ford and M. A. Deibel, *Anal. Chem.*, 2005, **77**, 1207–1215.
25 R. Haddad, R. Sparrapan and M. N. Eberlin, *Rapid Commun. Mass Spectrom.*, 2006, **20**, 2901–2905.
26 M. Himmelsbach, M. Waser and C. Klampfl, *Anal. Bioanal. Chem.*, 2014, **406**, 3647–3656.
27 P. J. Roach, J. Laskin and A. Laskin, *Analyst*, 2010, **135**, 2233–2236.
28 K. G. Asano, M. J. Ford, B. A. Tomkins and G. J. van Berkel, *Rapid Commun. Mass Spectrom.*, 2005, **19**, 2305–2312.
29 J. L. Zhang, Z. G. Zhou, J. W. Yang, W. Zhang, Y. Bai and H. W. Liu, *Anal. Chem.*, 2012, **84**, 1496–1503.
30 M. Resano, E. G. Ruiz, V. G. Mihucz, A. M. Moricz, G. Zaray and F. Vanhaecke, *J. Anal. At. Spectrom.*, 2007, **22**, 1158–1162.
31 J. Chirinos, D. Oropeza, J. Gonzalez, M. Ranaudo and R. E. Russo, *Energy Fuels*, 2013, **27**, 2431–2436.
32 J. Laskin, B. S. Heath, P. J. Roach, L. Cazares and O. J. Semmes, *Anal. Chem.*, 2012, **84**, 141–148.
33 V. L. Dorofeev, A. A. Konovalov, V. Y. Kochin and A. P. Arzamastsev, *Pharm. Chem. J.*, 2004, **38**, 510–512.
34 M. J. Walworth, J. J. Stankovich, G. J. van Berkel, M. Schulz, S. Minarik, J. Nichols and E. Reich, *Anal. Chem.*, 2011, **83**, 591–597.
35 J. Gasparic, *Adv. Chromatogr.*, 1992, **31**, 153–252.

